

## Early Fermi Gamma-ray Space Telescope Observations of the Quasar 3C 454.3

A. A. Abdo<sup>1,2</sup>, M. Ackermann<sup>3</sup>, M. Ajello<sup>3</sup>, W. B. Atwood<sup>4</sup>, M. Axelsson<sup>5,6</sup>, L. Baldini<sup>7</sup>,  
 J. Ballet<sup>8</sup>, G. Barbiellini<sup>9,10</sup>, D. Bastieri<sup>11,12</sup>, M. Battelino<sup>5,13</sup>, B. M. Baughman<sup>14</sup>,  
 K. Bechtol<sup>3</sup>, R. Bellazzini<sup>7</sup>, B. Berenji<sup>3</sup>, R. D. Blandford<sup>3</sup>, E. D. Bloom<sup>3</sup>,  
 E. Bonamente<sup>15,16</sup>, A. W. Borgland<sup>3</sup>, A. Bouvier<sup>3</sup>, J. Bregeon<sup>7</sup>, A. Brez<sup>7</sup>, M. Brigida<sup>17,18</sup>,  
 P. Bruel<sup>19</sup>, T. H. Burnett<sup>20</sup>, G. A. Caliendo<sup>17,18</sup>, R. A. Cameron<sup>3</sup>, P. A. Caraveo<sup>21</sup>,  
 J. M. Casandjian<sup>8</sup>, E. Cavazzuti<sup>22</sup>, C. Cecchi<sup>15,16</sup>, E. Charles<sup>3</sup>, S. Chaty<sup>8</sup>,  
 A. Chekhtman<sup>23,2</sup>, C. C. Cheung<sup>24</sup>, J. Chiang<sup>3</sup>, S. Ciprini<sup>15,16</sup>, R. Claus<sup>3</sup>,  
 J. Cohen-Tanugi<sup>25</sup>, L. R. Cominsky<sup>26</sup>, J. Conrad<sup>5,13,27,28</sup>, L. Costamante<sup>3</sup>, S. Cutini<sup>22</sup>,  
 C. D. Dermer<sup>2</sup>, A. de Angelis<sup>29</sup>, F. de Palma<sup>17,18</sup>, S. W. Digel<sup>3</sup>, E. do Couto e Silva<sup>3</sup>,  
 D. Donato<sup>24</sup>, P. S. Drell<sup>3</sup>, R. Dubois<sup>3</sup>, D. Dumora<sup>30,31</sup>, C. Farnier<sup>25</sup>, C. Favuzzi<sup>17,18</sup>,  
 W. B. Focke<sup>3</sup>, L. Foschini<sup>32</sup>, M. Frailis<sup>29</sup>, L. Fuhrmann<sup>33</sup>, Y. Fukazawa<sup>34</sup>, S. Funk<sup>3</sup>,  
 P. Fusco<sup>17,18</sup>, F. Gargano<sup>18</sup>, D. Gasparrini<sup>22</sup>, N. Gehrels<sup>24,35</sup>, S. Germani<sup>15,16</sup>, B. Giebels<sup>19</sup>,  
 N. Giglietto<sup>17,18</sup>, P. Giommi<sup>22</sup>, F. Giordano<sup>17,18</sup>, T. Glanzman<sup>3</sup>, G. Godfrey<sup>3</sup>,  
 I. A. Grenier<sup>8</sup>, M.-H. Grondin<sup>30,31</sup>, J. E. Grove<sup>2</sup>, L. Guillemot<sup>30,31</sup>, S. Guiriec<sup>36</sup>,  
 Y. Hanabata<sup>34</sup>, A. K. Harding<sup>24</sup>, R. C. Hartman<sup>24</sup>, M. Hayashida<sup>3</sup>, E. Hays<sup>24</sup>,  
 R. E. Hughes<sup>14</sup>, G. Jóhannesson<sup>3</sup>, A. S. Johnson<sup>3</sup>, R. P. Johnson<sup>4</sup>, W. N. Johnson<sup>2</sup>,  
 T. Kamae<sup>3</sup>, H. Katagiri<sup>34</sup>, J. Kataoka<sup>37</sup>, N. Kawai<sup>38,39</sup>, M. Kerr<sup>20</sup>, J. Knödseder<sup>40</sup>,  
 M. L. Kocian<sup>3</sup>, F. Kuehn<sup>14</sup>, M. Kuss<sup>7</sup>, L. Latronico<sup>7</sup>, S.-H. Lee<sup>3</sup>, M. Lemoine-Goumard<sup>30,31</sup>,  
 F. Longo<sup>9,10</sup>, F. Loparco<sup>17,18</sup>, B. Lott<sup>30,31,56</sup>, M. N. Lovellette<sup>2</sup>, P. Lubrano<sup>15,16</sup>,  
 G. M. Madejski<sup>3,56</sup>, A. Makeev<sup>23,2</sup>, E. Massaro<sup>53</sup>, M. N. Mazziotta<sup>18</sup>, J. E. McEnery<sup>24</sup>,  
 S. McGlynn<sup>5,13</sup>, C. Meurer<sup>5,27</sup>, P. F. Michelson<sup>3</sup>, W. Mitthumsiri<sup>3</sup>, T. Mizuno<sup>34</sup>,  
 A. A. Moiseev<sup>41,35</sup>, C. Monte<sup>17,18</sup>, M. E. Monzani<sup>3</sup>, A. Morselli<sup>42</sup>, I. V. Moskalenko<sup>3</sup>,  
 S. Murgia<sup>3</sup>, P. L. Nolan<sup>3</sup>, J. P. Norris<sup>43</sup>, E. Nuss<sup>25</sup>, T. Ohsugi<sup>34</sup>, N. Omodei<sup>7</sup>, E. Orlando<sup>44</sup>,  
 J. F. Ormes<sup>43</sup>, D. Paneque<sup>3</sup>, J. H. Panetta<sup>3</sup>, D. Parent<sup>30,31</sup>, V. Pelassa<sup>25</sup>, M. Pepe<sup>15,16</sup>,  
 M. Pesce-Rollins<sup>7</sup>, F. Piron<sup>25</sup>, T. A. Porter<sup>4</sup>, S. Rainò<sup>17,18</sup>, R. Rando<sup>11,12</sup>, M. Razzano<sup>7</sup>,  
 A. Reimer<sup>3</sup>, O. Reimer<sup>3</sup>, T. Reposeur<sup>30,31</sup>, L. C. Reyes<sup>45</sup>, S. Ritz<sup>24,35</sup>, L. S. Rochester<sup>3</sup>,  
 A. Y. Rodriguez<sup>46</sup>, F. Rahoui<sup>8</sup>, F. Ryde<sup>5,13</sup>, H. F.-W. Sadrozinski<sup>4</sup>, R. Sambruna<sup>24</sup>,  
 D. Sanchez<sup>19</sup>, A. Sander<sup>14</sup>, P. M. Saz Parkinson<sup>4</sup>, J. D. Scargle<sup>55</sup>, C. Sgrò<sup>7</sup>, M. S. Shaw<sup>3</sup>,  
 D. A. Smith<sup>30,31</sup>, P. D. Smith<sup>14</sup>, G. Spandre<sup>7</sup>, P. Spinelli<sup>17,18</sup>, J.-L. Starck<sup>8</sup>,  
 M. S. Strickman<sup>2</sup>, D. J. Suson<sup>47</sup>, H. Tajima<sup>3</sup>, H. Takahashi<sup>34</sup>, T. Takahashi<sup>48</sup>, T. Tanaka<sup>3</sup>,  
 J. B. Thayer<sup>3</sup>, J. G. Thayer<sup>3</sup>, D. J. Thompson<sup>24</sup>, L. Tibaldo<sup>11,12</sup>, D. F. Torres<sup>49,46</sup>,  
 G. Tosti<sup>15,16</sup>, A. Tramacere<sup>50,3</sup>, Y. Uchiyama<sup>3</sup>, T. L. Usher<sup>3</sup>, N. Vilchez<sup>40</sup>, M. Villata<sup>54</sup>,  
 V. Vitale<sup>42,51</sup>, A. P. Waite<sup>3</sup>, B. L. Winer<sup>14</sup>, K. S. Wood<sup>2</sup>, T. Ylinen<sup>52,5,13</sup>, J. A. Zensus<sup>33</sup>,  
 M. Ziegler<sup>4</sup>

*Submitted to the Astrophysical Journal*

---

<sup>1</sup>National Research Council Research Associate

<sup>2</sup>Space Science Division, Naval Research Laboratory, Washington, DC 20375

<sup>3</sup>W. W. Hansen Experimental Physics Laboratory, Kavli Institute for Particle Astrophysics and Cosmology, Department of Physics and SLAC National Accelerator Laboratory, Stanford University, Stanford, CA 94305

<sup>4</sup>Santa Cruz Institute for Particle Physics, Department of Physics and Department of Astronomy and Astrophysics, University of California at Santa Cruz, Santa Cruz, CA 95064

<sup>5</sup>The Oskar Klein Centre for Cosmo Particle Physics, AlbaNova, SE-106 91 Stockholm, Sweden

<sup>6</sup>Department of Astronomy, Stockholm University, SE-106 91 Stockholm, Sweden

<sup>7</sup>Istituto Nazionale di Fisica Nucleare, Sezione di Pisa, I-56127 Pisa, Italy

<sup>8</sup>Laboratoire AIM, CEA-IRFU/CNRS/Université Paris Diderot, Service d’Astrophysique, CEA Saclay, 91191 Gif sur Yvette, France

<sup>9</sup>Istituto Nazionale di Fisica Nucleare, Sezione di Trieste, I-34127 Trieste, Italy

<sup>10</sup>Dipartimento di Fisica, Università di Trieste, I-34127 Trieste, Italy

<sup>11</sup>Istituto Nazionale di Fisica Nucleare, Sezione di Padova, I-35131 Padova, Italy

<sup>12</sup>Dipartimento di Fisica “G. Galilei”, Università di Padova, I-35131 Padova, Italy

<sup>13</sup>Department of Physics, Royal Institute of Technology (KTH), AlbaNova, SE-106 91 Stockholm, Sweden

<sup>14</sup>Department of Physics, Center for Cosmology and Astro-Particle Physics, The Ohio State University, Columbus, OH 43210

<sup>15</sup>Istituto Nazionale di Fisica Nucleare, Sezione di Perugia, I-06123 Perugia, Italy

<sup>16</sup>Dipartimento di Fisica, Università degli Studi di Perugia, I-06123 Perugia, Italy

<sup>17</sup>Dipartimento di Fisica “M. Merlin” dell’Università e del Politecnico di Bari, I-70126 Bari, Italy

<sup>18</sup>Istituto Nazionale di Fisica Nucleare, Sezione di Bari, 70126 Bari, Italy

<sup>19</sup>Laboratoire Leprince-Ringuet, École polytechnique, CNRS/IN2P3, Palaiseau, France

<sup>20</sup>Department of Physics, University of Washington, Seattle, WA 98195-1560

<sup>21</sup>INAF-Istituto di Astrofisica Spaziale e Fisica Cosmica, I-20133 Milano, Italy

<sup>22</sup>Agenzia Spaziale Italiana (ASI) Science Data Center, I-00044 Frascati (Roma), Italy

<sup>23</sup>George Mason University, Fairfax, VA 22030

<sup>24</sup>NASA Goddard Space Flight Center, Greenbelt, MD 20771

<sup>25</sup>Laboratoire de Physique Théorique et Astroparticules, Université Montpellier 2, CNRS/IN2P3, Montpellier, France

<sup>26</sup>Department of Physics and Astronomy, Sonoma State University, Rohnert Park, CA 94928-3609

- 
- <sup>27</sup>Department of Physics, Stockholm University, AlbaNova, SE-106 91 Stockholm, Sweden
- <sup>28</sup>Royal Swedish Academy of Sciences Research Fellow, funded by a grant from the K. A. Wallenberg Foundation
- <sup>29</sup>Dipartimento di Fisica, Università di Udine and Istituto Nazionale di Fisica Nucleare, Sezione di Trieste, Gruppo Collegato di Udine, I-33100 Udine, Italy
- <sup>30</sup>CNRS/IN2P3, Centre d'Études Nucléaires Bordeaux Gradignan, UMR 5797, Gradignan, 33175, France
- <sup>31</sup>Université de Bordeaux, Centre d'Études Nucléaires Bordeaux Gradignan, UMR 5797, Gradignan, 33175, France
- <sup>32</sup>INAF Osservatorio Astronomico di Brera, I-23807 Merate, Italy
- <sup>33</sup>Max-Planck-Institut für Radioastronomie, Auf dem Hügel 69, 53121 Bonn, Germany
- <sup>34</sup>Department of Physical Sciences, Hiroshima University, Higashi-Hiroshima, Hiroshima 739-8526, Japan
- <sup>35</sup>University of Maryland, College Park, MD 20742
- <sup>36</sup>University of Alabama in Huntsville, Huntsville, AL 35899
- <sup>37</sup>Waseda University, 1-104 Totsukamachi, Shinjuku-ku, Tokyo, 169-8050, Japan
- <sup>38</sup>Cosmic Radiation Laboratory, Institute of Physical and Chemical Research (RIKEN), Wako, Saitama 351-0198, Japan
- <sup>39</sup>Department of Physics, Tokyo Institute of Technology, Meguro City, Tokyo 152-8551, Japan
- <sup>40</sup>Centre d'Étude Spatiale des Rayonnements, CNRS/UPS, BP 44346, F-30128 Toulouse Cedex 4, France
- <sup>41</sup>Center for Research and Exploration in Space Science and Technology (CRESST), NASA Goddard Space Flight Center, Greenbelt, MD 20771
- <sup>42</sup>Istituto Nazionale di Fisica Nucleare, Sezione di Roma “Tor Vergata”, I-00133 Roma, Italy
- <sup>43</sup>Department of Physics and Astronomy, University of Denver, Denver, CO 80208
- <sup>44</sup>Max-Planck Institut für extraterrestrische Physik, 85748 Garching, Germany
- <sup>45</sup>Kavli Institute for Cosmological Physics, University of Chicago, Chicago, IL 60637
- <sup>46</sup>Institut de Ciències de l'Espai (IEEC-CSIC), Campus UAB, 08193 Barcelona, Spain
- <sup>47</sup>Department of Chemistry and Physics, Purdue University Calumet, Hammond, IN 46323-2094
- <sup>48</sup>Institute of Space and Astronautical Science, JAXA, 3-1-1 Yoshinodai, Sagamihara, Kanagawa 229-8510, Japan
- <sup>49</sup>Institució Catalana de Recerca i Estudis Avançats (ICREA), Barcelona, Spain
- <sup>50</sup>Consorzio Interuniversitario per la Fisica Spaziale (CIFS), I-10133 Torino, Italy
- <sup>51</sup>Dipartimento di Fisica, Università di Roma “Tor Vergata”, I-00133 Roma, Italy
- <sup>52</sup>School of Pure and Applied Natural Sciences, University of Kalmar, SE-391 82 Kalmar, Sweden

## ABSTRACT

This is the first report of Fermi Gamma-ray Space Telescope observations of the quasar 3C 454.3, which has been undergoing pronounced long-term outbursts since 2000. The data from the Large Area Telescope (LAT), covering 2008 July 7–October 6, indicate strong, highly variable  $\gamma$ -ray emission with an average flux of  $\sim 3 \times 10^{-6}$  photons  $\text{cm}^{-2} \text{s}^{-1}$ , for energies  $> 100$  MeV. The  $\gamma$ -ray flux is variable, with strong, distinct, symmetrically-shaped flares for which the flux increases by a factor of several on a time scale of about three days. This variability indicates a compact emission region, and the requirement that the source is optically thin to pair-production implies relativistic beaming with Doppler factor  $\delta > 8$ , consistent with the values inferred from VLBI observations of superluminal expansion ( $\delta \sim 25$ ). The observed  $\gamma$ -ray spectrum is not consistent with a simple power-law, but instead steepens strongly above  $\sim 2$  GeV, and is well described by a broken power-law with photon indices of  $\sim 2.3$  and  $\sim 3.5$  below and above the break, respectively. This is the first direct observation of a break in the spectrum of a high luminosity blazar above 100 MeV, and it is likely direct evidence for an intrinsic break in the energy distribution of the radiating particles. Alternatively, the spectral softening above 2 GeV could be due to  $\gamma$ -ray absorption via photon-photon pair production on the soft X-ray photon field of the host AGN, but such an interpretation would require the dissipation region to be located very close ( $\lesssim 100$  gravitational radii) to the black hole, which would be inconsistent with the X-ray spectrum of the source.

*Subject headings:* Galaxies: active – quasars: individual: 3C 454.3 – Gamma rays: observations

## 1. Introduction

The successful launch on 2008 June 11 of the Gamma-ray Large Area Space Telescope (GLAST) — now known as the Fermi Gamma-ray Space Telescope — ushered in a new

---

<sup>53</sup>Dipartimento di Fisica, Università di Roma “La Sapienza”, Piazzale A. Moro 2, I-00185, Roma, Italy

<sup>54</sup>INAF, Osservatorio Astronomico di Torino, Italy

<sup>55</sup>Space Science Division, NASA/Ames Research Center, Moffet Field, CA 94035-1000

<sup>56</sup>*Corresponding authors:* Greg Madejski, [madejski@slac.stanford.edu](mailto:madejski@slac.stanford.edu), and Benoit Lott, [lott@cenbg.in2p3.fr](mailto:lott@cenbg.in2p3.fr)

era of observational astronomy in the energetic  $\gamma$ -ray band. Early observations (including those conducted during in-orbit checkout) proved that the performance of the Large Area Telescope (LAT; for details see Atwood et al. 2009), sensitive in the band 20 MeV to  $> 300$  GeV, has been close to the pre-flight predictions (Abdo et al. 2008). The data obtained with the EGRET instrument on-board the Compton Gamma-ray Observatory, LAT’s predecessor, indicated that the most prominent extragalactic energetic  $\gamma$ -ray sources are blazars, a sub-class of active galactic nuclei whose overall flux is dominated by emission from a relativistically boosted inner ( $\leq$  pc) jet. Here, we use an example of early LAT observations of the blazar, 3C 454.3, to highlight the capabilities of the instrument, but also to derive further constraints on the emission mechanisms and structure of the object.

Observationally, blazars are characterized by large amplitude chaotic variability measured in all accessible spectral bands, from radio to GeV or even TeV energies. The variability often manifests itself as very high flux states that last for months to years, with more rapid, smaller amplitude flares superimposed on those high states. Optical and radio data show a high degree of polarization, and the radio data reveal the presence of strong emission components that arise from extremely compact ( $\sim$  milliarcsec), spatially and spectrally variable structures with a core-jet morphology, often associated with apparent superluminal expansion.

3C 454.3, at redshift  $z = 0.859$ , is a well-known example of this class of objects. Long-term VLBI monitoring indicates a jet Lorentz factor of  $\Gamma_{\text{jet}} = 15.6 \pm 2.2$ , an angle of motion to our line-of-sight of  $\theta = 1.3 \pm 1.2^\circ$ , and a corresponding Doppler factor of  $\delta \equiv (\Gamma_{\text{jet}}(1 - \beta \cos \theta))^{-1} \sim 25$  (Jorstad et al. 2005). These values are consistent with recent work by Lister et al. (2009). This object entered a high-flux phase in 2000 and was remarkably active in 2005, when it reached the largest apparent optical luminosity ever recorded from an astrophysical source apart from GRBs (Fuhrmann et al. 2006; Villata et al. 2006). The 2005 outburst was covered also in the X-ray range by the Swift satellite (Giommi et al. 2006). Unfortunately, due to the lack of contemporaneous  $\gamma$ -ray data, no firm conclusions could be drawn regarding the bolometric energetics of 3C 454.3 during this outburst. Historically, the source was detected above 100 MeV by EGRET (Hartman et al. 1999), and in the softer  $\gamma$ -ray bands by OSSE (McNaron-Brown et al. 1995) and COMPTEL (Zhang et al. 2005). The  $\gamma$ -ray flux measured by the AGILE satellite in 2007, when the source was optically fainter than in 2005 but much brighter than during its low states (Ghisellini et al. 2007; Vercellone et al. 2008; 2009), was much higher than the  $\gamma$ -ray flux recorded by EGRET during low states (see Raiteri et al. 2008 for multi-band data). This indicates that the synchrotron (optical) outbursts in 3C 454.3 are indeed generally accompanied by  $\gamma$ -ray outbursts. In particular, the AGILE observations found an average flux of  $F_{E>100\text{MeV}} = 2.8 \pm 0.4 \times 10^{-6}$  photons  $\text{cm}^{-2} \text{s}^{-1}$  in 2007 July 24–30 (Vercellone et al. 2008), and a flux of  $1.7 \pm 0.13 \times 10^{-6}$  photons  $\text{cm}^{-2} \text{s}^{-1}$

in 2007 November 10–December 1, with the spectrum well-described by a power law with photon index  $\Gamma = 1.73 \pm 0.16$  (Vercellone et al. 2009). The MAGIC telescope also observed but did not detect 3C 454.3 at TeV energies during these epochs; the non-detection implies a spectral cut-off at  $\sim 20$  GeV (Anderhub et al. 2008).

As expected, 3C 454.3 was detected easily by Fermi (Tosti et al. 2008). Owing to its high flux state, it was possible for the LAT to measure its variability properties on time scales of less than a day. The  $\gamma$ -ray observations by the LAT are described in Section 2. Given the strong and variable  $\gamma$ -ray flux, simultaneous data were highly desirable, and we secured a number of observations in the radio, optical, and X-ray bands. We report on some of those results here, although more detailed inter-band timing correlations will be the subject of a future paper. In Section 3, we present the overall spectrum of the source and compare the  $\gamma$ -ray variability properties to those measured in other bands. There, we also present an emission model for the source and highlight the new constraints derived from our data. We summarize our findings in Section 4.

## 2. Observations

### 2.1. LAT Data: Light curve and $\gamma$ -ray spectrum

The LAT (Atwood et al. 2009) simultaneously monitors  $\sim 2.4$  steradians on the sky, albeit with an effective area that varies significantly with the arrival direction of the incident photon with respect to the instrument pointing direction. In survey mode, the instrument z-axis is offset  $35^\circ$  North and South from the spacecraft zenith during alternate orbits in order to provide complete sky coverage every three hours. The LAT instrument was turned on 2008 June 25, and the data presented here were collected during the early check-out phase (which ended on August 11) until October 6. Most data were taken in survey mode, the source being observed at an average off-axis angle of  $37^\circ$ . The effective area decreases to about 80% and 70% of the on-axis value at  $30^\circ$  and  $40^\circ$  respectively. About 7000 photons with  $E > 100$  MeV ascribed to 3C 454.3 were detected during the continuous survey mode extending from August 4 to October 6. The exposure at 1 GeV for this period was  $\simeq 6.5 \times 10^5$  m<sup>2</sup>s.

For the period July 7–July 31, the instrument was alternately pointed at two sky regions centered on Vela and 3EG J1835+5918. In the later case, 3C 454.3 was observed with an average off-axis angle of  $55^\circ$ , i.e., close to the edge of the field-of-view, with a corresponding reduction of the effective area of about 50% with respect to the on-axis value.

The light curve obtained with the LAT is shown in Figure 1. We used the standard

LAT analysis software, `ScienceTools v9r7`<sup>57</sup>, and performed a maximum likelihood fit of the model parameters. The source model included a point source for 3C 454.3, a component for the Galactic diffuse emission derived using the GALPROP code (Strong, Moskalenko, & Reimer 2004; Strong et al. 2004), and an isotropic component to represent, in combination, the extragalactic diffuse emission and the residual instrument background. The spectral shape of the isotropic component was derived from high Galactic latitude ( $|b| > 60^\circ$ ) sky survey data accumulated over a similar time period as the data for 3C 454.3. The events were selected using the most stringent set of standard analysis cuts and correspond to the so-called “diffuse class” events, which comprise the highest quality photon events in terms of direction and energy reconstruction and background rejection. The events were extracted in the range 100 MeV–300 GeV and within a  $15^\circ$  acceptance cone centered on the location of 3C 454.3. This region is substantially larger than the 68% containment angle of the PSF at the lowest energies ( $\sim 3^\circ$ ). This is necessary in order to constrain the diffuse emission components accurately. Since the likelihood calculation models the spatial distribution of events as a function of energy, this procedure naturally accounts for the narrower PSF at higher energies when fitting the point source spectral parameters.

We note that 3C 454.3 was sufficiently bright that the background contribution within a few degrees of the source is only a small fraction of the source count rate and that the observed flux variations of the source do not correlate with the changing background level along the satellite orbit. Our current estimate of systematics is  $< 20\%$  on the flux.

Figure 1 shows that the source is consistently variable, with the rise and decay times of  $\sim 3.5$  days, corresponding to the doubling of the flux in 2 days. The spectral shape appears constant during this period within the systematic uncertainties. The flux  $F_{E>100\text{MeV}}$  peaks at roughly  $1.2 \times 10^{-5}$  photons  $\text{cm}^{-2} \text{s}^{-1}$  on MJD 54657 (2008 July 10). Note that such an exceptional flux from any blazar was only observed twice during the EGRET era, for 3C 279 (Wehrle et al. 1998) and PKS 1622-297 (Mattox et al. 1997). In survey mode, the relative change of reconstructed flux due to uncorrected acceptance variations (calibration of the effective area as a function of the off-axis angle) has been determined to be about 5% for a daily light curve using the data from the (steady) bright pulsars. An additional 15% uncertainty has been estimated to affect the data collected in pointing mode presented here, because of the proximity of the source direction to the edge of the field of view.

We have also fit the broad-band spectrum of the combined data from the onset of the regular survey mode, August 3, through September 2. As with the daily light curve analysis, we have used the standard “diffuse” class event selections and restricted the energy range

---

<sup>57</sup><http://fermi.gsfc.nasa.gov/ssc/data/analysis/documentation/Cicerone/>

to 200 MeV–300 GeV. Since 3C 454.3 has consistently been one of the brightest sources since the beginning of the mission, the data accumulated over the month of survey data are sufficient to allow us to consider models that are more complex than a simple power-law in trying to fit the source spectrum.

Our basic model does use a simple power-law for 3C 454.3, and that model yields a photon index of  $\Gamma = 2.40 \pm 0.03_{\text{stat}} \pm 0.09_{\text{sys}}$ . This is substantially *softer* than the index reported by AGILE, but the data were not contemporaneous. The difference could also be partially due to different bandpasses of the two instruments. The residuals to the power-law fit clearly indicate that the spectral model for the  $\gamma$ -ray emission from 3C 454.3 must be more complex; and in particular, the data show a steepening towards higher energies. A broken power-law model yields  $\Gamma_{\text{low}} = 2.27 \pm 0.03_{\text{stat}} \pm 0.09_{\text{sys}}$ ,  $\Gamma_{\text{high}} = 3.5 \pm 0.2_{\text{stat}} \pm 0.15_{\text{sys}}$ , and a break energy of  $2.4 \pm 0.3_{\text{stat}} \pm 0.3_{\text{sys}}$  GeV. The likelihood ratio test gives the probability for incorrectly rejecting the power-law model in favor of the broken power-law model as  $5 \times 10^{-12}$ . The break was consistently detected at similar energies when repeating the analysis for different one-month periods (Aug., Sep., Oct.). An instrumental effect can safely be ruled out, given the level of the systematic uncertainties. An unfolded  $\nu F_\nu$  spectrum corresponding to this model is shown in Figure 2. We note that with the current data, we cannot distinguish between various models describing the steepening spectrum, e.g., broken power-law vs. exponentially cut-off power-law, but such differentiation might be possible with more data. Nonetheless, this is the first indication of an observed break in the  $\gamma$ -ray spectrum of a high luminosity blazar, calling for a complex spectral model beyond a simple power-law approximation. With this model, we determine the time-averaged flux for the 2008 August 3 – September 4 epoch to be  $F_{E>100\text{MeV}} = 3.0 \pm 0.1 \times 10^{-6}$  photons  $\text{cm}^{-2} \text{s}^{-1}$ .

## 2.2. Low Energy Observations

Triggered by the detection of a high flux level during the first intensive Fermi-LAT observations of 3C 454.3 in 2008 July/August, the broad-band behavior of the source was monitored via an ad-hoc multi-wavelength (MW) campaign covering the period 2008 July to 2009 January. These intensive observations involved ground-based monitoring at radio cm/mm/sub-mm wavelengths (e.g., Effelsberg 100-m, IRAM 30-m, SMA and OVRO 40-m telescopes) and at IR/optical bands (e.g., Spitzer, Kanata/Hiroshima 1.5-m and REM telescopes, plus telescopes of the GASP-WEBT consortium). In addition, daily 2 ksec observations were performed with the Swift satellite, providing X-ray data, as well as optical and UV coverage. Details of this multi-wavelength campaign, including all collected data and the corresponding MW analysis of the source behavior between 2008 June and 2009

January at radio/IR/optical/UV/X-ray/ $\gamma$ -ray bands, will be presented in a subsequent paper (Abdo et al. 2009, in preparation). For the purpose of the first LAT results presented here, we will use a sub-set of these MW data to construct a quasi-simultaneous spectral energy distribution of 3C 454.3 including radio, optical, UV, X-ray and LAT  $\gamma$ -ray data. In Figure 3, we show the corresponding data collected during the period MJD 54685–54690 (2008 August 7–12).

The radio cm/mm band data were obtained with the Effelsberg 100-m and IRAM 30-m telescopes in the framework of a Fermi-related monitoring program of potential  $\gamma$ -ray blazars (F-GAMMA project, Fuhrmann et al. 2007). At Effelsberg, observations were conducted quasi-simultaneously at eight frequencies between 2.6 and 42 GHz using cross-scans in azimuth and elevation direction. Consequently, pointing off-set correction, gain correction, atmospheric opacity correction and sensitivity correction have been applied to the data (for details see Fuhrmann et al. 2008 and Angelakis et al. 2008). The observations at the IRAM 30-m telescope were obtained with SIS receivers (operating at 86, 142 and 228 GHz) and with calibrated cross-scans in azimuth and elevation direction. The receiver calibration was done using hot and cold loads (standard chopper wheel method) and the opacity corrected intensities were converted into the standard temperature scale. After Gauss fitting of the averaged sub-scans, each temperature was corrected for remaining pointing offsets and systematic gain-elevation effects. The conversion to the standard flux density scale was done using the instantaneous conversion factors derived from primary calibrator measurements (for details, see Ungerechts et al. 1998).

The optical, UV, and soft X-ray data were obtained from 2 ksec pointings with the Swift satellite as a part of daily TOO observations during the campaign. For the screening, reduction and analysis of the data from Swift instruments we used standard procedures within the HEASoft v. 6.5 software package with the calibration database updated as of 2008 June 26. The XRT operated in photon counting mode, and the analysis was performed with the `xrtpipeline` task with default parameters and having selected photons with grades 0–12. We also checked for the presence of pile-up. The UVOT data were integrated with the `uvotimsum` task and analyzed with the `uvotsource` task using source region radii of 5'' for the optical filters and 10'' for the UV filters, respectively. The background was extracted from a nearby source-free circular region with 50'' radius. The observed magnitudes were converted into flux densities according to standard procedures (Poole et al. 2008).

### 3. Discussion

#### 3.1. Overall Spectral Energy Distribution and Modeling of the Source

The amplitude of blazar variability can be as high as a factor of 100, so many important inferences with regard to the source structure can be derived most robustly from broad band spectra obtained simultaneously, with additional, crucial constraints from time-resolved broad-band spectroscopy. To this end, we assembled the data as given above, contemporaneous with our 2008 August epoch. We plot a quasi-simultaneous spectral energy distribution (SED) using our MW data from August 7–12 in Figure 3. The overall SED of the source is broadly similar to that observed for other EGRET blazars, revealing two broad peaks: one in the mm-to-IR band and the other in the  $\gamma$ -ray band. Given the polarization measured in all accessible segments of the low energy component, the most viable emission mechanism is the synchrotron process, produced by a distribution of relativistic electrons radiating in an ambient magnetic field.

The high energy peak, in turn, could be due to Compton scattering of either the synchrotron photons internal to the jet (see, e.g., Ghisellini, Maraschi, & Treves 1985) or the radiation associated with the nucleus, such as the photons produced by the accretion disk, broad emission line region, or the thermal emission produced by the circumnuclear dust in the host galaxy (Dermer, Schlickeiser, & Mastichiadis 1992; Sikora, Begelman, & Rees 1994). Radiation from ultra-high energy protons or ions that interact with magnetic fields associated with the jet or its environment, including subsequent cascades, may be an alternative explanation for the high energy component (e.g., Mücke et al. 2003; Atoyan & Dermer 2003; Böttcher, Reimer, & Marscher 2008).

Inferences regarding the source structure are strongly model-dependent, even within leptonic emission models. A comparison of results presented for 3C 454.3 in Vercellone et al. (2009) with the analysis of the broad-band temporal behavior of Sikora et al. (2008) clearly indicates that a wide range of parameters can describe the same data. Nonetheless, the different models do find roughly consistent values of the jet Doppler factor,  $\delta \sim 25$ , the magnetic field,  $B \sim 1$  Gauss, and the Lorentz factors of the electrons that radiate the bulk of the observed power,  $\gamma_{\max} \sim 10^3$ . The largest disparity arises in the distance,  $r$ , of the dissipation region from the central black hole (i.e., the location of the “blazar emission zone”), and this points to differing origins of the seed photons that are Compton up-scattered to the  $\gamma$ -ray range: UV disk photons reprocessed in the broad line region vs. IR emission of the obscuring dust. In particular, Vercellone et al. claim  $r \sim 3 \times 10^{16}$  cm, while Sikora et al. argue for  $r \sim 10^{19}$  cm. As we discuss below, our detection of the spectral break can put further constraints on the location of dissipation region, but ultimately, time-resolved broad

band spectroscopy will be crucial.

### 3.2. Implications of the $\gamma$ -ray Variability on the Lorentz Factor of the Source of the $\gamma$ -ray emission

The  $\gamma$ -ray flux from 3C 454.3 is clearly variable on time scales ranging from days to decades, with the average flux value measured during the LAT observations being somewhat higher than that found by AGILE and much higher than that measured by EGRET. Assuming a “concordance” cosmology ( $\Omega_\Lambda = 0.73$ ,  $\Omega_{\text{matter}} = 0.27$ , and  $H_0 = 71 \text{ km s}^{-1} \text{ Mpc}^{-1}$ ), we infer a luminosity distance of  $d_L = 5.5 \text{ Gpc}$  and an apparent isotropic monochromatic luminosity of  $L_{E_0} \approx 4\pi d_L^2 (\Gamma_{\text{low}} - 1) E_0 F_{E>E_0} \approx 2 \times 10^{48} \text{ erg s}^{-1}$ , where  $E_0 = 100 \text{ MeV}$  and we have used the average 2008 August 3–September 4 flux of  $F_{E_0} = 3.0 \times 10^{-6} \text{ ph cm}^{-2} \text{ s}^{-1}$ . The bolometric luminosity is expected to be much higher than this since the high-energy spectral component peaks below 100 MeV. This finding, together with the observed rapid, large amplitude variability measured in the  $\gamma$ -ray band, puts strong constraints on the source parameters. If a stationary source of a given luminosity in  $\gamma$ -rays and X-rays were to be as compact as one would infer from the variability data, the source would be optically thick to  $e^+/e^-$  pair production, assuming that the X-ray emission is co-spatial with the the  $\gamma$ -ray emission. This assumption is justified by the simultaneity of the flaring activity in both bands as observed during our MW campaign, and in particular, as seen from our full Swift XRT soft X-ray TOO observations (2008 July–September; Abdo et al. 2009, in preparation). Similar simultaneous X-ray/ $\gamma$ -ray variability has been measured in the past for other sources, such as 3C 279 (Wehrle et al. 1998).

One obvious solution to the problem of excess pair-production opacity is to invoke relativistic motion and/or expansion of the source. Following the arguments given in Mattox et al. (1993, with corrections pointed out in Madejski et al. 1996), and adopting the doubling time scale of  $t_d \approx 2 \text{ days}$  and the observed X-ray flux of  $S_X \approx 3 \times 10^{-11} \text{ erg cm}^{-2} \text{ s}^{-1}$  (as measured during our campaign) at the observed photon frequency  $\nu_X \approx 10^{18} \text{ Hz}$  (corresponding to the photons that annihilate with the GeV  $\gamma$ -rays in the jet rest frame), we estimate the Doppler factor  $\delta$  required for the photon-photon annihilation optical depth to be  $\tau_{\gamma\gamma} \leq 1$ . With the derived relation  $\tau_{\gamma\gamma} \sim \sigma_T d_L^2 S_X / 3 t_d c^2 E_X \delta^4$ , where we put the emission region linear size  $R = c t_d \delta / (1 + z)$ , the source-frame photon energy  $E'_X = (1 + z) h \nu_X / \delta$ , and the intrinsic X-ray luminosity  $L'_X = 4\pi d_L^2 \delta^{-4} S_X$ , one obtains  $\delta \gtrsim 8$  (note here that the estimated Doppler factor scales as  $\delta \propto t_d^{-1/4}$ ). Of course, omitting the requirement of co-spatiality of the X-ray and  $\gamma$ -ray emission regions relaxes this limit. Nonetheless, it is interesting to compare this constraint on the Doppler factor with the estimate obtained from

the VLBI superluminal motion,  $\delta = 24.6 \pm 4.5$  (Jorstad et al. 2005). As long as the velocity of the VLBI jet is the same as the velocity of the outflow within the blazar emission zone, this implies that the photon-photon annihilation effects involving the X-ray emission generated within the jet are negligible.

### 3.3. Implications of the Complex $\gamma$ -ray Spectrum

The LAT data imply a more complex spectrum than a simple power-law, indicating significant softening of the photon spectral index by  $\Delta\Gamma \sim 1.2$  towards higher energies. This is not consistent with a spectral change of  $\Delta\Gamma = 0.5$  that is expected from the typical “cooling break” associated with radiative losses. The observed softening may instead be due to an intrinsic decline or break in the particle distribution. It can also arise, at least partially, from “environmental” reasons, i.e., the underlying photon spectrum is modified by the photon-photon pair production. For 3C 454.3, this is unlikely to be due to the intergalactic diffuse background light (EBL) which would only affect the spectra from a source at  $z \leq 1$  at energies  $\geq 40$  GeV. Also, as argued above, the pair-production effects internal to the jet are negligible, since the expected jet Doppler factor ( $\delta \sim 25$ ) is much larger than that required for internal  $\gamma$ -ray transparency ( $\delta \gtrsim 8$ ). A photon field that is external to the jet but local to the blazar central engine would need to peak at  $\sim 0.2$  keV in order to account for the observed spectral softening at  $\sim 2$  GeV. This requirement would exclude photons produced in the Broad Line Region (BLR) as the source of pair opacity since that emission peaks in the UV. However, the required X-ray photons could be produced in the innermost part of the putative accretion disk surrounding the central black hole and/or a hot corona above the disk.

We do not know the shape of the intrinsic, unabsorbed  $\gamma$ -ray spectrum, but the simplest assumption is that it is a straight power-law, as is believed to be produced via 1st-order Fermi acceleration at shocks. Departures from such a spectral shape may involve both softening and hardening towards higher energies over the canonical power-law component, arising due to radiative particle energy losses and/or efficient stochastic acceleration acting near the shock front (see, e.g. Stawarz & Petrosian 2008). For a simple power-law, we can estimate the opacity that the emerging  $\gamma$ -rays would encounter as a function of distance from the black hole, given the observed spectral break at 2 GeV (e.g., Reimer 2007). Assuming crudely that the break corresponds to the location where the pair-production opacity  $\tau$  is of order unity, we can estimate the *minimum* distance at which the  $\gamma$ -rays are produced. We consider the soft X-ray target photons at  $\sim 0.2$  keV as being produced either in the inner parts of an accretion disk (assumed here to follow the behavior of a Shakura-Sunyaev disk spectrum) or

in an X-ray emitting hot corona above the disk. For a black hole mass estimate for 3C 454.3 of  $4 \times 10^9 M_\odot$  (Gu et al. 2001) and a mass accretion rate of  $\sim 10\%$  the Eddington rate, the bolometric (Shakura-Sunyaev) disk luminosity would be  $L_{\text{bol}} \sim 2 \times 10^{46} \text{ erg s}^{-1}$ . This is in good agreement with reports from Raiteri et al. (2007) of the quiet state UV-spectrum of 3C 454.3 that shows a rise in the SED, suggesting the onset of the “big blue bump” thermal accretion disk spectrum. It is also in good agreement with the luminosity estimate of the BLR from Pian et al. (2006) of order  $L_{\text{BLR}} \sim 3 \times 10^{45} \text{ erg s}^{-1}$ , implying a typical covering factor of  $\sim 10\%$ . The interaction of jet GeV photons with soft X-ray photons originating in the inner parts of an accretion disk implies photon-photon interactions at preferentially small angles. The angular dependence of the threshold target photon energy,  $E_{\text{thr}} = (2m_e c^2)^2 / (2E_\gamma(1 - \cos \theta))$ , where  $\theta$  is the interaction angle, requires correspondingly higher densities of energetic target photons than are expected to be emitted by a standard Shakura-Sunyaev disk around a  $4 \times 10^9 M_\odot$  black hole for which the thermal emission is weak at 0.2 keV and above.

On the other hand, quasars often show soft X-ray emission extending up to  $\sim 100$  keV that is believed to arise from Comptonization by a hot coronal plasma above the disk. This mechanism creates a characteristic flat continuum that can typically be modeled as an  $E^{-2}$  photon spectrum with an exponential cut-off at  $\sim 100$  keV. Rapid variability of this flux indicates that it is emitted within the regions closest to the black hole. Adopting the typical values of the ratio  $L_X/L_{\text{bol}}$  of 1–10% (Laor et al. 1997), we find that the condition corresponding to a unity optical depth for 2 GeV photons occurs at  $r \lesssim 10^{-3}\text{--}10^{-2}$  pc, corresponding to  $\sim 10\text{--}100$  gravitational radii for  $M_{\text{BH}} = 4 \times 10^9 M_\odot$ . Thus, if the observed spectral break at 2 GeV were due to photon-photon pair production on the accretion disc corona radiation, the implied location of the  $\gamma$ -ray emitting region should be extremely close to the black hole. Another scenario can be envisioned in which radiation from the accretion disk corona is subsequently Thomson-scattered towards the jet by the free electrons in the gas in the more distant broad line region. However, this would require an unrealistically high product of covering fraction and Thomson optical depth that would not be consistent with the observed profiles of emission lines in AGN unless the electrons were located well within the broad-line region. Regardless, neither direct nor BLR-scattered accretion disk corona radiation are likely sources of the required pair opacity, because the reprocessed  $\gamma$ -radiation should then escape as soft and strong X-ray emission produced in a pair cascade developed in the intense photon field of the accretion disk/disk corona (Levinson & Blandford 1995; Ghisellini & Madau 1996), which is not consistent with the collected X-ray data in the context of the broad-band spectrum (see. e.g., Fig. 3).

We thus suggest that the observed 2 GeV break in the  $\gamma$ -ray spectrum of 3C 454.3 is due to an intrinsic break in the spectrum of radiating particles. In the context of models

invoking Comptonization of external photons, such a break implies a characteristic Lorentz factor,  $\gamma_{\text{el}}$ , for the electrons radiating at the break. For inverse-Compton scattering of “seed” photons that have energy  $E_{\text{seed,rest}}$  in the rest frame of the blazar, the observed  $\gamma$ -ray photon energy is given by

$$E_{\gamma} = E_{\text{seed,rest}} \delta \Gamma_{\text{jet}} (1 + z)^{-1} \gamma_{\text{el}}^2. \quad (1)$$

Hence, the Lorentz factor of electrons radiating at  $E_{\gamma} = 2 \text{ GeV}$  is

$$\gamma_{\text{el}} \approx 6 \times 10^3 (\delta/10)^{-1/2} (\Gamma_{\text{jet}}/10)^{-1/2} (E_{\text{seed,rest}}/\text{eV})^{-1/2} \quad (2)$$

The likely sources of seed photons in blazars are either UV photons from the accretion disk that are reprocessed in the BLR and which comprise primarily Ly $\alpha$  photons with  $E_{\text{seed,rest}} \sim 10 \text{ eV}$ , or IR emission from obscuring dust which have  $E_{\text{seed,rest}} \sim 0.3 \text{ eV}$ . These seed photon energies yield  $\gamma_{\text{el}} \sim 10^3$  and  $\sim 6 \times 10^3$ , for the cases of UV or IR seed photons, respectively, assuming the kinematic jet parameters  $\delta = 25$  and  $\Gamma_{\text{jet}} = 15$  as inferred from VLBI observations. In principle, for those values of  $\gamma_{\text{el}}$ , the  $\gamma$ -ray radiation is close to the onset of the Klein-Nishina (KN) regime, but as has been argued by several authors (Zdziarski & Krolik 1993; Moderski et al. 2005), such a KN cut-off might be less severe than expected in the simplest scenarios. Regardless, we also comment here that such complex *intrinsic*  $\gamma$ -ray spectrum, if common, may present an obstacle towards the use of luminous blazars as “white light” sources to study the intergalactic diffuse UV/optical background radiation, first because it is not known whether the break can be reliably modeled, but also because the steepening spectrum reduces the photon statistics at the highest  $\gamma$ -ray energies, where the opacity of the diffuse background light is most pronounced. Finally, it is interesting to speculate about the issue of contribution of  $\gamma$ -ray - luminous blazars to the extragalactic  $\gamma$ -ray background. Specifically, if luminous blazars make a significant contribution to this background and if a spectral break at a few GeV is a common feature in such blazars, then evidence of such breaks should be present in the extragalactic diffuse emission. To settle this issue, sensitive, well-calibrated data extending to the highest energies accessible by Fermi are necessary, but detailed analysis of the diffuse extragalactic background in Fermi data is yet to be performed.

#### 4. Summary

We report strong and variable  $\gamma$ -ray emission from the blazar 3C 454.3 measured by the LAT instrument onboard the Fermi Gamma-ray Space Telescope. The source, in a flaring/active state since 2000, was easily detected and showed rapid variability described as symmetric flares with rise and fall time of  $\sim 3.5$  days, reaching a peak flux of  $F_{E>100\text{MeV}}$  of about  $1.2 \times 10^{-5} \text{ photons cm}^{-2} \text{ s}^{-1}$ . The time scales of those flares, coupled with the

X-ray luminosity of the jet, allow us to provide a lower limit on the Doppler factor of the jet of  $\delta > 8$ , consistent with the values inferred for much larger spatial scales with VLBI measurements.

We also find that the  $\gamma$ -ray spectrum of 3C 454.3 is not a simple power-law, but instead, steepens towards higher energies. A good, but not unique, description of the spectrum is a broken power-law with photon indices of  $\sim 2.3$  and  $\sim 3.5$ , below and above a break at  $\sim 2$  GeV, respectively. This break might be due to photon-photon absorption to pair production, but this would require the region responsible for production of  $\gamma$ -ray flux to be sufficiently close to the accretion disk/black hole system to produce spectral signatures of the reprocessed  $\gamma$ -rays in the X-ray photon energy range, which are not observed. Instead, we propose that an intrinsic break in the electron spectrum around electron energies  $E_{\text{el}}$  of  $\sim 10^3 m_e c^2$  is a more likely explanation for the observed  $\gamma$ -ray spectral shape.

**Acknowledgments:** The *Fermi* LAT Collaboration acknowledges generous ongoing support from a number of agencies and institutes that have supported both the development and the operation of the LAT as well as scientific data analysis. These include the National Aeronautics and Space Administration and the Department of Energy in the United States, the Commissariat à l’Energie Atomique and the Centre National de la Recherche Scientifique / Institut National de Physique Nucléaire et de Physique des Particules in France, the Agenzia Spaziale Italiana and the Istituto Nazionale di Fisica Nucleare in Italy, the Ministry of Education, Culture, Sports, Science and Technology (MEXT), High Energy Accelerator Research Organization (KEK) and Japan Aerospace Exploration Agency (JAXA) in Japan, and the K. A. Wallenberg Foundation, the Swedish Research Council and the Swedish National Space Board in Sweden. Additional support for science analysis during the operations phase from the following agencies is also gratefully acknowledged: the Istituto Nazionale di Astrofisica in Italy and the K. A. Wallenberg Foundation in Sweden for providing a grant in support of a Royal Swedish Academy of Sciences Research fellowship. SLAC researchers acknowledge the support by the US Department of Energy contract DE-AC02-76SF00515 to the SLAC National Accelerator Laboratory. This research is partly based on observations with the 100-m telescope of the MPIfR (Max-Planck-Institut für Radioastronomie) at Effelsberg. This paper is partly based on observations carried out at the 30-m telescope of IRAM, which is supported by INSU/CNRS (France), MPG (Germany) and IGN (Spain). Finally, we also acknowledge many fruitful discussions with Drs. L. Stawarz and M. Sikora.

## REFERENCES

Abdo, A., et al. 2008, accepted by ApJ (arXiv:0812.2960)

- Anderhub, H., et al. 2008, M., submitted to A&A (arXiv:0811.1680)
- Atoyan, A. & Dermer, C. D., 2003, ApJ, 586, 79
- Atwood, W., et al. 2009, submitted to ApJ (arXiv:0902:1089)
- Böttcher, M., Reimer, A., & Marscher, A. 2008, submitted to ApJ (arXiv:0810.4864)
- Dermer, C. D., Schlickeiser, R., & Mastichiadis, A. 1992, A&A, 256, L27
- Fuhrmann, L., et al. 2006, A&A, 445, L1
- Fuhrmann, L., Zensus, J. A., Krichbaum, T. P., Angelakis, E., & Readhead, A. C. S. 2007, The First GLAST Symposium, 921, 249
- Fuhrmann, L., et al. 2008, A&A, 490, 1019
- Ghisellini, G., & Madau, P. 1996, MNRAS, 280, 67
- Ghisellini, G., Maraschi, L., & Treves, A. 1985, A&A, 146, 204
- Ghisellini, G., et al. 2007, MNRAS, 382, L82
- Giommi, P., et al. 2006 A&A 456, 911
- Gu, M., Cao, X., & Jiang, D. R. 2001, MNRAS, 327, 1111
- Hartman, R., et al. 1999, ApJS, 123, 79
- Jorstad, S., et al. 2005, AJ, 130, 1418
- Laor, A., et al. 1997, ApJ, 477, 93
- Levinson, A., & Blandford, R. 1995, ApJ, 449, 86
- Lister, M., et al. 2009 (arXiv:0902.2087)
- Madejski, G., et al. 1996, ApJ, 459, 156
- McNaron-Brown, K., et al. 1995, ApJ, 451, 575
- Mattox, J., et al. 1993, ApJ, 410, 609
- Mattox, J., et al. 1997, ApJ, 476, 692
- Moderski, R., Sikora, M., Coppi, P., & Aharonian, F. 2005, MNRAS, 363, 954

- Mücke, A., et al. 2003, *A&A*, 18, 593
- Pian, E., et al. 2006, *A&A*, 449, 21
- Poole, T. S., et al. 2008, *MNRAS*, 383, 627
- Raiteri, C., et al. 2007, *A&A*, 473, 819
- Raiteri, C., et al. 2008, *A&A*, 485, L17
- Reimer, A. 2007, *ApJ*, 665, 1023
- Sikora, M., Begelman, M. C., & Rees, M. J. 1994, *ApJ*, 421, 153
- Sikora, M., Moderski, R., & Madejski, G. M. 2008, *ApJ*, 675, 71
- Stawarz, L., & Petrosian, V. 2008, *ApJ*, 681, 1725
- Strong, A. W., Moskalenko, I. V., & Reimer, O. 2004, *ApJ*, 613, 962
- Strong, A. W., Moskalenko, I. V., Reimer, O., Digel, & S., Diehl, R. 2004, *A&A*, 422, L47
- Tosti, G., et al. 2008, *The Astronomer’s Telegram*, 1628, 1
- Ungerechts, H., et al. 1998, *IAU Colloq. 164: Radio Emission from Galactic and Extragalactic Compact Sources*, 144, 149
- Vercellone, S., et al. 2008, *ApJ*, 676, L13
- Vercellone, S., et al. 2009, *ApJ*, 690, 1018
- Villata, M., et al. 2006, *A&A*, 453, 817
- Wehrle, A., et al. 1998, *ApJ* 497, 178
- Zdziarski, A., & Krolik, J. 1993, *ApJ*, 409, L33
- Zhang, S., Collmar, W., & Schönfelder, V. 2005, *A&A*, 444, 767

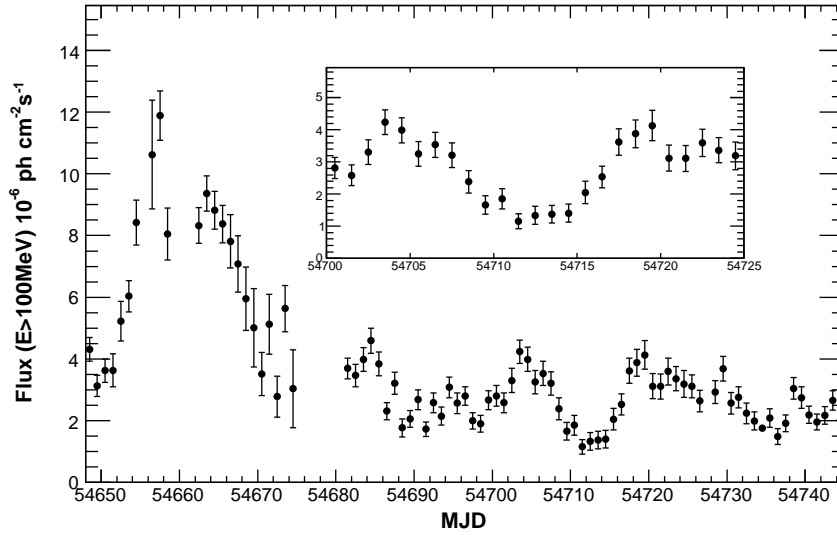


Fig. 1.— The flux light curve of 3C 454.3 in the 100 MeV–300 GeV band. The LAT operated in survey mode throughout these observations except during the period MJD 54654–54681 (2008 July 7–August 2), when it operated in pointed mode. The inset shows a blow up of the period MJD 54700–54725. The error bars are statistical only.

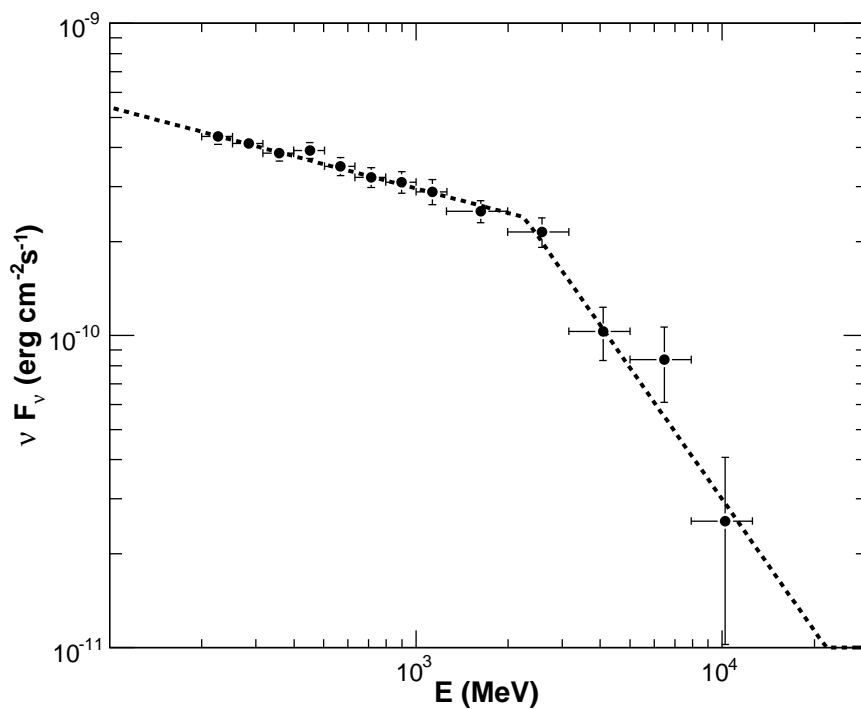


Fig. 2.—  $\nu F_\nu$  distribution of the summed Fermi LAT data over the 2008 August 3–September 2 time span. The model, fitted over the 200 MeV – 300 GeV range, is a broken power-law with photon indices  $\Gamma_{\text{low}} = 2.27 \pm 0.03$ ,  $\Gamma_{\text{high}} = 3.5 \pm 0.3$ , and a break energy  $E_{\text{br}} = 2.4 \pm 0.3$  GeV, and the apparent isotropic  $E > 100$  MeV luminosity of  $4.6 \times 10^{48}$  erg  $\text{cm}^{-2} \text{s}^{-1}$ . The error bars are statistical only.

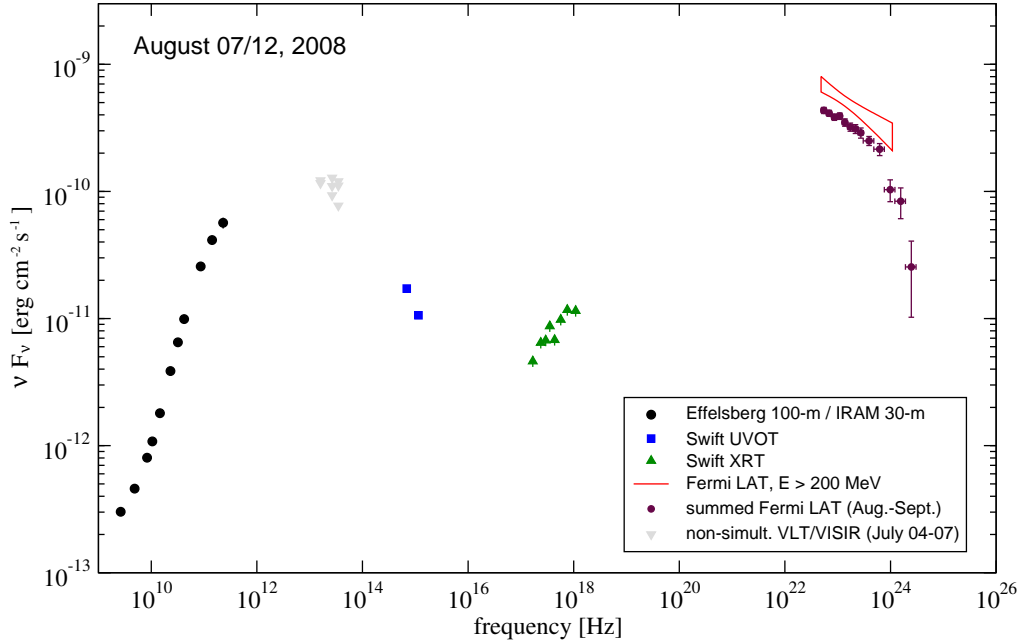


Fig. 3.— Broad-band, (quasi-) simultaneous spectral energy distribution of 3C 454.3 obtained during the period MJD 54685–54690 (2008 August 7–12). The MW data are part of a larger follow-up campaign triggered by the early Fermi LAT results. Here, we show radio cm/mm band observations (2.6 to 230 GHz) obtained with the Effelsberg 100-m and IRAM 30-m telescopes. The optical, UV and soft X-ray data were obtained from a 2 ksec pointing with the Swift satellite (UVOT, XRT) as part of daily TOO observations during the campaign (see Sect. 2.2 for details). For the  $\gamma$ -rays, the butterfly plot corresponds to the MJD 54685 (2008 August 7) data, while the points correspond to the August data as in Fig. 2. For illustration we also superimpose non-simultaneous mid-IR data obtained with the VLT/VISIR instruments during early 2008 July. Given the wide range of parameters that can reproduce the previously observed SEDs of 3C454.3 (see Section 3.1), we refrain from any detailed modeling, noting only that a hybrid synchrotron + external radiation Compton models can reproduce this SED adequately, and that the discrimination amongst details of various models requires time-resolved spectroscopy.